RSC Advances

This is an *Accepted Manuscript*, which has been through the Royal Society of Chemistry peer review process and has been accepted for publication.

Accepted Manuscripts are published online shortly after acceptance, before technical editing, formatting and proof reading. Using this free service, authors can make their results available to the community, in citable form, before we publish the edited article. This *Accepted Manuscript* will be replaced by the edited, formatted and paginated article as soon as this is available.

You can find more information about *Accepted Manuscripts* in the Information for Authors.

Please note that technical editing may introduce minor changes to the text and/or graphics, which may alter content. The journal's standard Terms & Conditions and the Ethical guidelines still apply. In no event shall the Royal Society of Chemistry be held responsible for any errors or omissions in this *Accepted Manuscript* or any consequences arising from the use of any information it contains.

ROYAL SOCIETY OF CHEMISTRY

www.rsc.org/advances

Self-assembly of folic acid/melamine complexes with hierarchy levels: from membranes to porous spherulites and networks

Pengyao Xing[a], Xiaoxiao Chu[a], Mingfang Ma[a], Shangyang Li[a], Yimeng Zhang[a] and Aiyou Hao[*a]

[a]*School of Chemistry and Chemical Engineering and Key Laboratory of Colloid and Interface Chemistry of Ministry of Education, Shandong University, Jinan 250100, PR China.*

RSC Advances Accepted Manuscript

* Fax: +86 531 88564464; Tel: +86 531 88363306; E-mail: haoay@sdu.edu.cn.

Abstract:

We report a hierarchical self-assembly shown by the complexation of folic acid and melamine in water. With the increase in folic acid (FA) concentration, 2D membranes, 0D spherulites and 3D networks with porous structures are constructed. H-bonds and π-π stacking interaction are proven to be the basic driving forces in the formation of membrane and plates with high inter-affinity, which further self-organize into anisotropic spherulites that show strong birefringence. When the concentration of FA further increases, crosslinked networks with high viscoelasticity will generate.

Introduction:

Self-assembled soft materials with various hierarchy levels, including 0D vesicles/spheres, 1D fibers/tubes, 2D membranes and 3D networks have attracted considerable attentions due to their amazing features and wide applications.[1] For fabricating soft materials used in medical and life sciences, people often pay attention to nature which is superior and more complicated than artificial systems.[2] In this way, polypeptides, DNA, polysaccharide/cyclodextrins, vitamins or other biotins have been investigated as building blocks to build up functional materials in the past decades.[3] In contrast to the rationally designed molecules, it is rather difficult to obtain ordered aggregates from ubiquitous natural products, probably due to their multiple functional groups and complex molecular structures. In spite of the obstacles, a variety of self-assembled aggregates have been prepared using natural assemblers, to name a few, membranes from iron (III)/tannins,[4] well-defined nanoparticles from catechols[5]. However, the fabrication of hierarchical self-assemblies of multi-dimensional

RSC Advances Accepted Manuscript

materials from natural products still remains challenging.[3-5]

Membranes play a significant role in maintaining the cellar shape and biological components in biological issues. Membrane-based materials show potential for sensing, catalysis, etc., and attract people's attention due to their biological applications.[6] Membranous aggregates (films, vesicles, ribbons) also show the possibility of topological transformation (hierarchical self-assembly) into other dimensional aggregates such as tubes, 3D networks.[7] Spherulite is a kind of polycrystalline aggregates with a spherical shape.[8] Just like the membrane (such as liposome) self-assembled in cells, spherulites as polycrystals, are found not only in volcanic rocks, silicate minerals, metals and simple organic molecules, but also widely in living organisms like brain，muscle，nerve, blood and bile etc.[9] Thus, self-organized spherulites from natural assemblers are of great importance in biological/medical areas. Generally, spherulites are given by the process of polymer crystallization, but cooling down the melts of some small organic molecules gives rise to spherulites as well. Spherulites can be categorized optically using polarized light and exhibit characteristic properties (Maltese cross pattern). These features of spherulite endow it with amazing and useful applications, mainly in medical and the art areas.[10] For example, the nerve fibrils of people who get Alzheimer's disease or Parkinson's disease would accumulate into radial shperulites that can be detected conveniently by crossed polarizers.[11]

Folic acid (FA), as a vitamin, is a natural product which has been extensively studied due to its anti-tumor effect and G-quartet formation property.[12] FA and its

RSC Advances Accepted Manuscript

derivatives have been proven to be the effective building blocks in fabricating supramolecular gels, liquid crystals or other aggregates.[12, 13] However, due to the poor solubility, materials self-assembled in pure water by native FA have rarely been probed although native FA can gel DMSO/water mixtures as elucidated by Nandi[13a] and our group[13b]. The pterin ring moiety of FA provides A-D-A-D (A: acceptor; D: donor) H-bonding sites, and the carboxylic groups of glutamic acid moieties provide protons and H-bonding sites as well.[14] Therefore, FA probably can form complementary H-bonds with some molecules, such as melamine. Melamine (Mm) which contains 9 H-bonding sites of D-A-D arrays, has a slight solubility in water and acts as an effective co-assembler in assisting the self-assemblies of organic acids or pterin analogues like riboflavin in aqueous media.[15] For example, Liu and coworkers utilized Mm to tailor the size, self-assembled routes of nanotubes from a bola-type glutamic acid derivative[14a]; Nandi and coworkers contribute mostly to the Mm-participated supramolecular gels with controllable fluorescent emissions.[15] Herein, we report a hierarchical self-assembly of FA/Mm complexes in water, which give rise to membranes, spherulites and networks with the increase of FA concentrations (Scheme 1). Spherulites and networks exhibit porous structures that consist of micro-plates and rods. Such plates and rods are derived from the growth and folding of initial membranes, predicted by the topological revolutions. H-bonds, π-π stacking are the primary driving forces in the aggregate formation, whereas the radical growth of plates crystallized from super-cooling enables the formation of the outstanding spherulites.

RSC Advances Accepted Manuscript

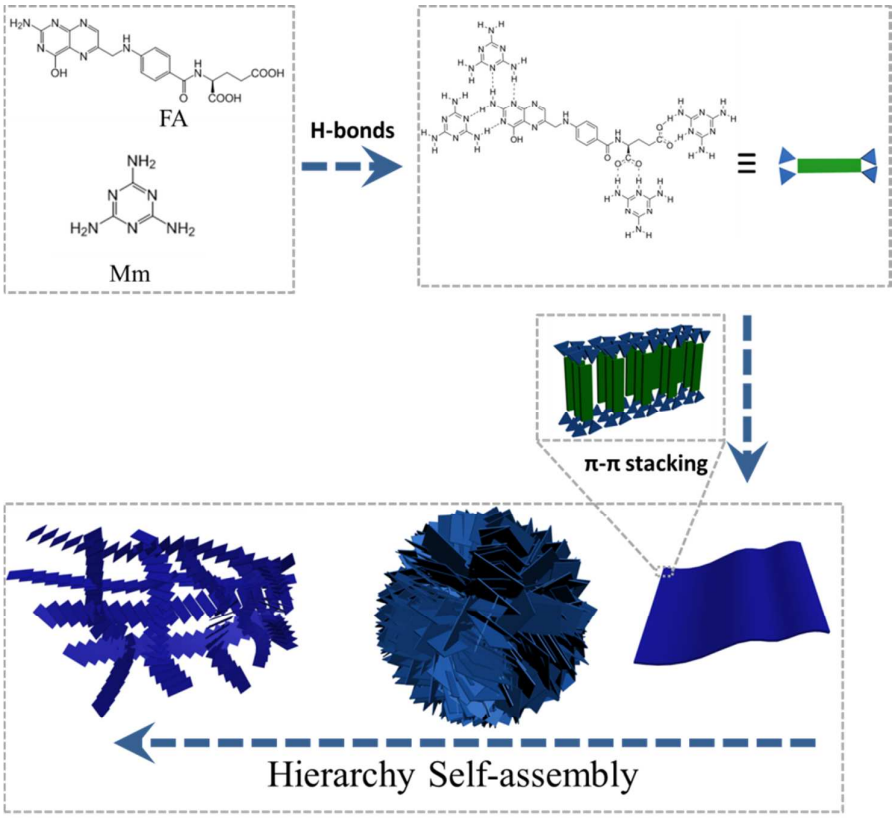

Scheme 1. Schematic representation of the hierarchical self-assembly of FA/Mm complexes.

Results and discussion

FA is almost insoluble (0.0016mg/ml) in water even at a high temperature. However, mixture of FA and Mm has a relatively high solubility (up to 4.0 mg/ml) at a high temperature (ca. 70 ^{o}C). Except for the low concentration range, FA can well dissolve in water at 70 ^{o}C only when ca. 3 equiv. (R = 3) or more Mm is added, indicating that FA provides multiple sites to interact with Mm. By cooling down the aqueous solutions of FA/Mm, aggregates with different macroscopic appearances were obtained. As shown in Fig. 1, transparent solutions, precipitates and viscous solutions would be obtained with the increase of FA concentration.

Those precipitates and viscous solutions were first performed on optical microscopy. It was found that, all the precipitates were actually composed of spherical

RSC Advances Accepted Manuscript

microparticles with multi-dispersity (Fig. 2 and Fig. S1). Under crossed polarizer, these spherical particles exhibited strong anisotropic birefringence. The well-defined Maltese cross patterns with blue and yellow colors indicate the formation of spherulites.[8-10] In the viscous solution phase, we also detected the presence of spherulites, which embedded in small size aggregates with barely birefringence (Fig. S1a-b'). If more than 10 equiv. Mm participates in the self-assembly, crystals of Mm would form, revealing an upper limit concentration of Mm. The formation of spherulites undergoes a nucleation-growth process, regulated by multiple factors such as concentration or cooling rate.[10] Under these circumstances, the spherulite sizes cannot be controlled precisely.

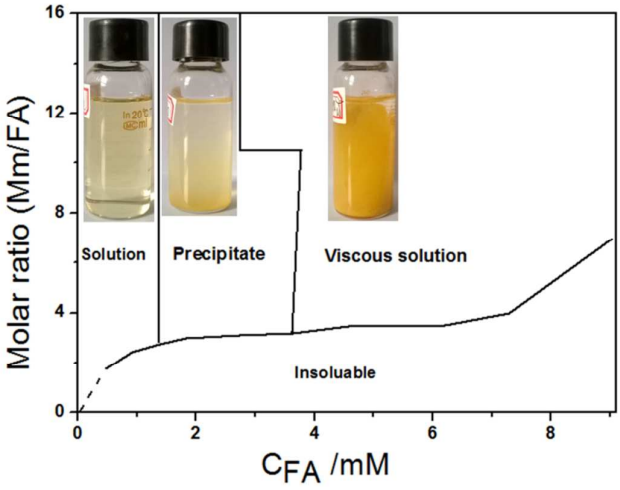

Figure 1. Phase diagram of the two component system. Insets: represented digital images of solution, precipitate and gel-like viscous solution. Dashed line: speculated boundary.

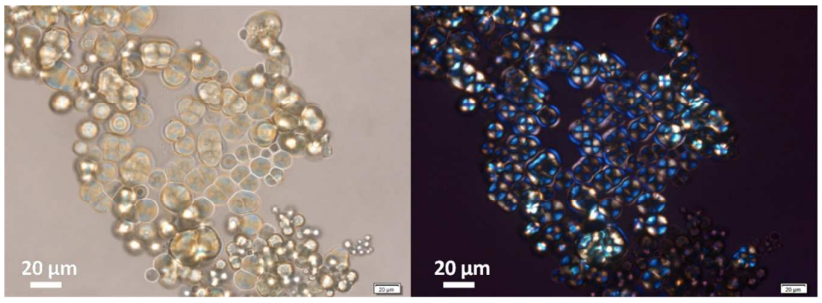

RSC Advances Accepted Manuscript

Figure 2. Optical microscopy images of precipitates (c_{FA} = 2 mM, R = 6) under natural and polarized light.

Then SEM experiments were carried out to probe the micro-morphologies of the self-assembled spherulites and viscous solutions. As displayed in Fig. 3 and Fig. S2-6, the surfaces of the spherulites are mainly composed of plates, which further self-assemble into porous structures with nanopockets. These particular morphologies show great similarity to graphene-based gels.[16] Notably, amongst the nanopockets, there are microrods exhibiting fibrous networks (red dashed circle of Fig. 3b, and Fig. S2-S3). The co-existence of microrods and microplates implies that, there would be two distinct self-assembly routes in the formation process of spherulites. Viscous solution samples display scattered microplates under SEM observations (Fig. S4). Similarly, the stacking of microplates affords the porous structure of viscous solutions. The common plate-like, porous feature of spherulite and networks well suggest the formation of hierarchical self-assembly. The thin-plates might be the basic building units in fabricating the spherical particles and infinite networks.

To confirm that hypothesis, TEM experiments which can provide insights into the inner structure of aggregates were performed. As shown in Figure 4, irregular micron-sized thin membranes are the dominant aggregates in solutions. The small size spherulites have the typical radical, porous structures, and this radical growth from nucleation sites reflects the category-one growing type.[17] The growth units, just as evidenced by SEM images, are membranes and nanorods. Unlike the spherulites, the membrane-encapsulated nanorods in viscous solution sample link together to give

RSC Advances Accepted Manuscript

networks (Fig. 4e, f). As shown in the dashed red squares, the initial spherulites and the initial networks share the same building units. It seems that, the nanorods are generated from the folding and overlapping of membranes. These structures collected from the bulk liquids are in good accordance with the SEM results, reflecting the hierarchical self-assembly process of FA/Mm complexes. These observations indicate that, the formation and growth of the initial membrane play a dominant role in tuning the topological morphologies.

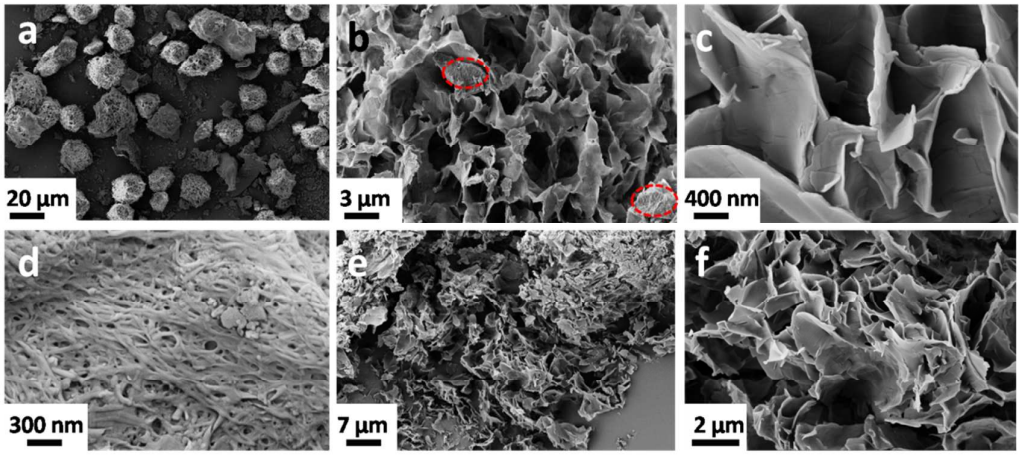

Figure 3. SEM images of spherulites (a-d, c: enlarged porous structures, d: enlarged images of red dashed circles) and networks (e-f).

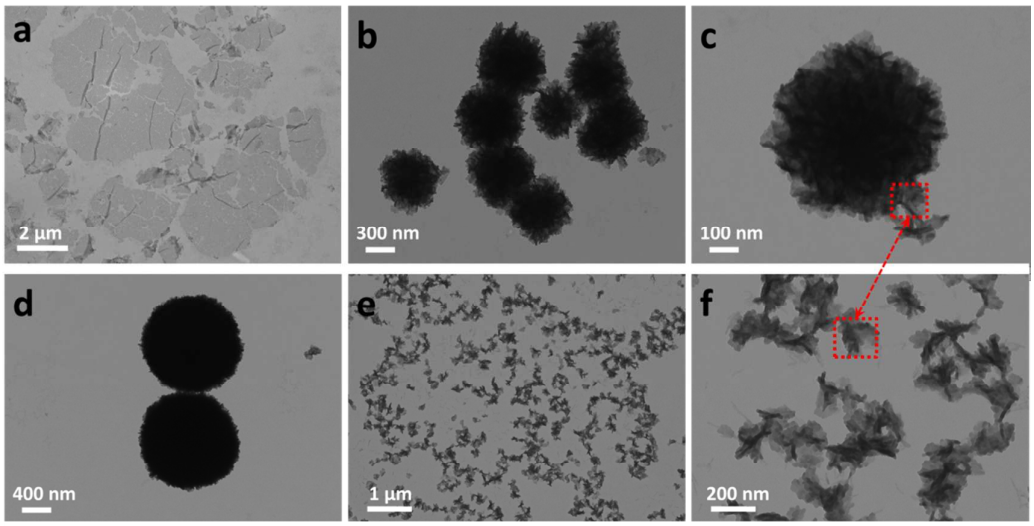

RSC Advances Accepted Manuscript

Figure 4. TEM images collected from the bulk phases of solution (a), precipitate (b-d) and viscous solution (e, f).

As stated in the last part, at high concentrations range, it would generate the viscous aggregate (inset of Fig. 1). We conducted the rheological experiments on the resultant viscous solutions. Frequency sweep indicates that, G′ (storage modulus) values of all performed samples are about one order of magnitude higher than that of G″ (loss modulus) over the entire range of applied frequencies. Moreover, both the G′ and G″ of samples display the frequency-independent behavior, indicating a solid-like behavior.[18] The complex viscosity linearly decreases against frequency sweep with a slope of -1. Therefore, the aggregates at high FA concentrations have highly viscoelastic properties (a hydrogel-like behavior).

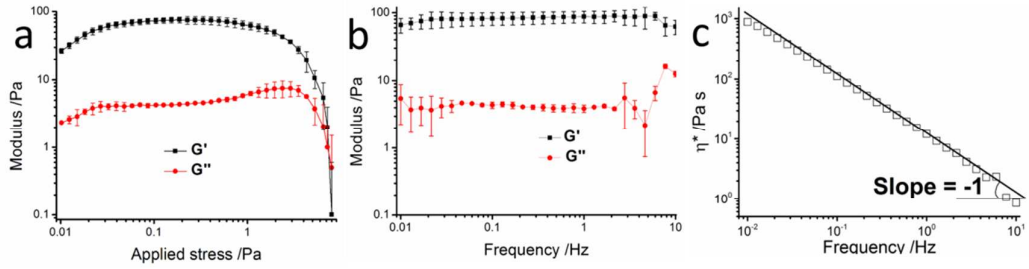

Figure 5. Dynamic oscillatory stress sweep (a, F = 1Hz), frequency sweep (b, applied stress = 1.0 Pa) and frequency dependency of the complex viscosity (c, applied stress = 1.0 Pa) of a high concentration sample (9 mM with 9 equiv. Mm).

Figure 6 displays the TGA and DSC curves of samples with different FA concentrations and molar ratios. The first weight loss before ca. 100 ^{o}C is attributed to the evaporation of entrapped water. At 250-300 ^{o}C, a significant weight loss occurs due to the degradation/cleavage of hydroxyl, amine and carboxyl groups of

RSC Advances Accepted Manuscript

FA/Mm. In DSC curves, two endothermic peaks were observed attributed to water evaporation and group degradation. The peaks at around 300 ^{o}C show dependence on the FA concentrations and R values. With the increase of FA concentration or R value, the endothermic peaks will be elevated greatly (Fig. 6b). For example, sample of 1.8 mM (R = 3.5) has a peak at 280 ^{o}C, whereas it increases to ca. 330 ^{o}C when more Mm (R = 16) involves in the self-assembly. The appearance of this peak at higher temperatures implies a better thermal stability. Therefore, by increasing the FA concentration and R value, the thermal stability can be enhanced remarkably, may be due to a more compact structure. Effective proton transfer between Mm and FA might contribute greatly to this phenomenon.

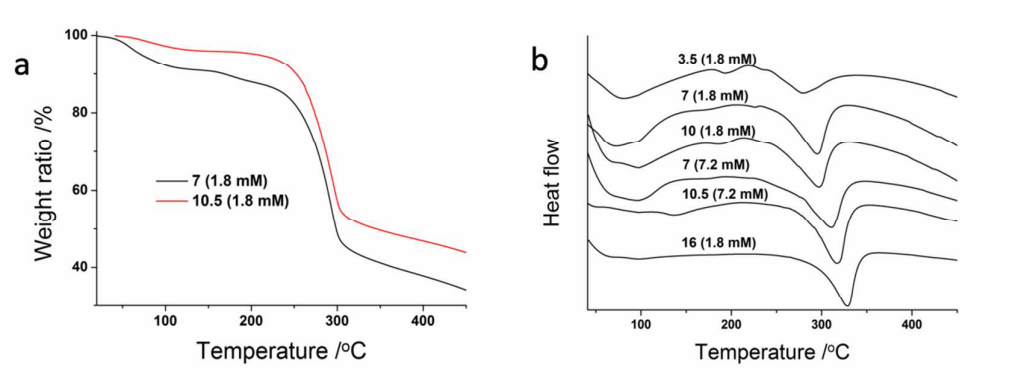

Figure 6. TGA and DSC curves of different samples. The marker means the R (c_{FA}).

Compared with the free molecule state in DMSO, UV-vis absorption peaks of FA/Mm complexes in water at 280 and 370 nm all show blue shifts (Figure 7a). Such blue shifts reflect a typical H-aggregate that contains face-to-face stacking arrays of FA molecules.[19] Hence, the chromophores of FA would be π-π stacked in the self-organized structures. It can also be found that, after self-organization, the absorption bands are barely broadened compared to the disassembled state, suggesting

RSC Advances Accepted Manuscript

an ordered organization. With the increase of the complexes' concentrations, the aromatic protons of FA shift to higher field, confirming the π-π stacking interaction (Fig. 7b).

FT-IR was employed to further confirm the interactions between FA and Mm (Fig. 7c). Sharp peaks at 3469 and 3413 cm^{-1} are assigned to the $–NH_2$ vibration stretching band of Mm ring. After complexing with FA, these two bands' relative intensities of Mm decrease gradually, accompanied by the appearance of the broadened peak at 3350 cm^{-1}. This implies the formation of H-bonds between FA and Mm.[20] Moreover, the $–NH_2$ and –OH stretching peaks of native FA at 3553, 3416 and 3319 cm^{-1} are absent after aggregation, indicating that the pterin ring of FA forms H-bonds with Mm. The C=O stretching vibrations (1693 cm^{-1}) of free carboxylic acid disappear, suggesting that the proton transfer effect occurs between the entire carboxylic groups and Mm. Proton transfer between triazine ring nitrogen and carboxylic acids can also be evidenced by the changes of C=N vibration of melamine.[14] In addition, the symmetrical stretching vibration (νs) peak of carboxylate at 1392 cm^{-1} also supports the presence of intermolecular proton transfer. The peak of 1510 cm^{-1} is contributed by amide-II band, suggesting the formation of intermolecular H-bonds between amides of glutamic acid moieties of FA.[22]

XRD patterns could verify the above-mentioned viewpoints, as shown in Fig. 7d. For samples with low concentration and R value, the peaks are totally different with that of pure FA. Three new small peaks at 6.43, 9.08 and 12.88 ^{o} correspond to the 100, 110 and 111 planes of tetragonal molecular packing, indicating the molecular

RSC Advances Accepted Manuscript

arrangement of FA backbones (Scheme 1). However, peaks of 17.8 ^{o} and 26.3 ^{o} appear in self-assembled samples, ascribed to the π-π stacking between Mm molecules.[14] It should be noted that, for samples with high concentrations and R values, peaks that show great similarity to pure Mm start to emerge. Such peaks indicate the formation of Mm crystals, which are in good accordance with morphologies detected by SEM and OM. According to the XRD patterns, the crystals of Mm belong to monoclinic syngony, where 100 plane (2θ = 13.0 ^{o}) and aggregate's 111 plane (12.88 ^{o}) slightly overlap.

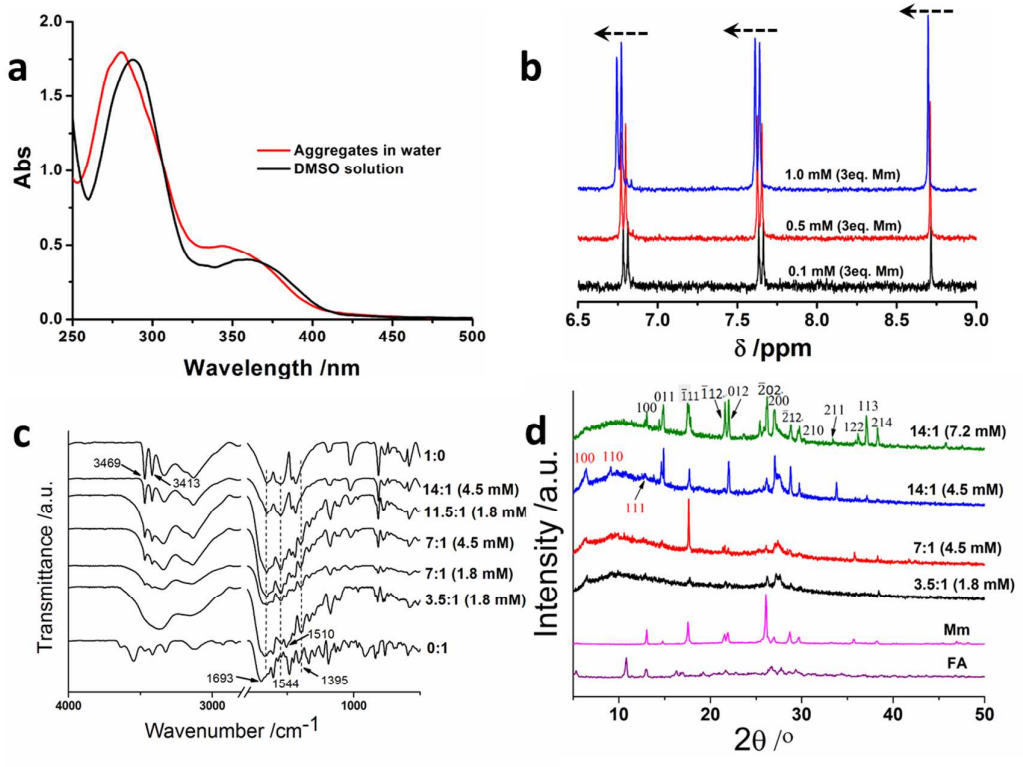

Figure 7. UV-vis spectra (a), selected ^{1}H NMR spectra (b), FT-IR spectra (c) and XRD patterns (d) of different samples; in d) the red hkl values stand for planes of aggregate while black hkl values stand for the planes of crystals.

Discussion

RSC Advances Accepted Manuscript

As elucidated above, we knew that Mm could interact with glutamic acid and pterin ring moieties of FA by complementary H-bonds and proton transfer. These interactions assist the self-assembly and contribute to a better solubility of FA in water. The outstanding hierarchical self-assembly or concentration-dependent typological revolution is clearly on the basis of membrane formation and growth. Moreover, the nucleation and growth play an essential role as well, *e.g.*, in the process of transition from graphene-like thin membranes to thick plates in spherulites or networks, from plates to radical spherulites with strong birefringence. Apart from the growth of membranes driven by the intermolecular π-π stacking and H-bonds, the formation of the particular rods might be due to the folding and overlap of initial membranes. This hypothesis can be proven to be valid, evidenced by the network-like membrane surface (Fig. S7) and their effective folds and overlaps (Fig. S8). These morphologies are similar to the nano- and microrods detected by SEM and TEM (Fig. 3, 4). According to the AFM results (Fig. 8), the surface of the membrane is rough, which is consistent with TEM observations. Also cross-section profile indicates that, the thickness of the membrane is ca. 2~3 nm, corresponding to the single molecular length of FA/Mm complexes. Furthermore, in the supernate of high concentration samples, we also observed the presence of some membrane-like aggregates with thickness of several nanometers (but with more regular shapes, Fig. S9), implying a similar self-assembly pathway in samples with different concentrations.

At ultralow concentrations, Mm interacts with FA to form H-bonded complexes which further π-π stacked into the very thin membranes. Due to the solution is highly

RSC Advances Accepted Manuscript

diluted, the inter-membrane interactions are too weak to further aggregate. But when the concentration increases, membranes form first, followed by the growth and folding to generate thicker membranes or plates which also act as nuclei to trigger the radical growth (spherulites). At high concentration range, more nanoplates or thicker membranes would form, which disfavors the radical growth but favors the linear growth to form networks. The networks are infinite aggregates and clearly have larger aggregation number than that of sperulites. According to the equation[22]:

$$\mu_N = \mu_\infty + \frac{\alpha kT}{N_p}$$

when the concentration increases, networks will form to generate a high aggregation number (N) which corresponds to a lower chemical potential. The low chemical potential means that, the networks are thermodynamic stable at high concentrations. On the other hand, when the concentration decreases, aggregation number will decrease to generate a higher chemical potential. The increased mean free energy per molecules will be compensated by the disappearance of networks' unfavorable rim energy to produce spherical aggregates.

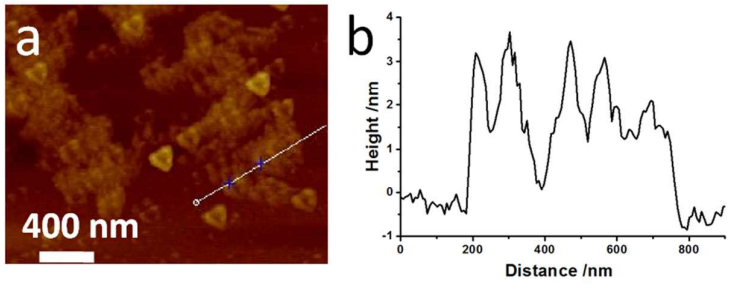

Fig. 8 AFM image (a) of the aggregates from diluted solution (1 mM, 3 equiv. Mm), b: cross-section profile from.

Another amazing feature of the FA/Mm self-assembly is the spherulite formation

RSC Advances Accepted Manuscript

owing to the fact that plate-like spherulites are rare, not to mention coming from natural small molecule. In contrast to the compact morphologies from the melts, open morphologies often occur in solution-growing spherulites. This theory is fine confirmed by the porous structure of the resultant FA/Mm spherulites. Super-cooling of super-saturated FA/Mm complex solutions provides a strong driving force for crystallization that is the prerequisite for spherulites. The networks hardly show birefringence, although spheres and networks own the same building units—microplates/rods. Therefore, the birefringence may be derived from the secondary self-organization or crystallization of microplates/membranes ascribed to their high affinities (electrostatic forces). This is in sharp contrast to the conventional polymeric spherulite formation. Though the details need to be further studied, this finding would broaden the concept and category of spherulites and self-assemblies.

Conclusions

In summary, FA/Mm complexes showed an outstanding hierarchical self-assembly that generates multiple dimensional aggregates at different concentration ranges. H-bonds and π-π stacking allow the formation of membranes, which further grow into plate-constituted spherulites and networks. Super-cooling of saturated FA/Mm solution enables the anisotropic growth (or crystallization) of plates and membranes to form spherulites with strong birefringence. Due to the secondary self-organization of the plates, spherulites and networks exhibit porous structures. Natural assemblers have opened a brand new path for advanced soft materials, and this system that shows multiple topological morphologies would greatly enrich the categories and concepts.

RSC Advances Accepted Manuscript

References

1 T. Sun, H. Yan, G. Liu, J. Hao, J. Su, S. Li, P. Xing and A Hao, *J. Phys. Chem. B*, 2012, **116**, 14628.; P. Xing, T. Sun and A. Hao, *RSC Adv*., 2013, **3**, 24776.; P. Gao, C. Zhan, L. Liu, Y. Zhou and M. Liu, *Chem. Commun*., 2004, 1174.; M. F. L. De Volder, S. H. Tawfick, R. H. Baughman and A. J. Hart, *Science*, 2013, **339**, 535.

2 W. E. Bentley and G. F. Payne, *Science*, 2013, **341**, 136.

3 H. Kang, H. Liu, X. Zhang, J. Yan, Z. Zhu, L. Peng, H. Yang, Y. Kim and W. Tan, *Langmuir*, 2011, **27**, 399.; X. Miao, W. Cao, W. Zheng, J. Wang, X. Zhang, J. Gao, C. Yang, D. Kong, H. Xu, L. Wang and Z. Yang, *Angew. Chem. Int. Ed*., 2013, **52**, 7781.; P. Xing, T. Sun, S. Li, A. Hao, J. Su and Y. Hou, *Colloids Surfaces A*, 2013, **421**, 44.; P. Xing, S. Li, F. Xin, Y. Hou, A. Hao, T. Sun and J. Su, *Carbohydr. Res*., 2013, **367**, 18.; P. Xing, X. Chu, S. Li, F. Xin, M. Ma and A. Hao, *New J. Chem*., 2013, **37**, 3949.; P. Xing, X. Chu, S. Li, Y. Hou, M. Ma, J. Yang and A. Hao, *RSC Adv*., 2013, **3**, 22087.; M. dIschia, A. Napolitano, A. Pezzella, P. Meredith and T. Sarna, *Angew. Chem. Int. Ed*., 2009, **48**, 3914.

4 H. Ejima, J. J. Richardson, K. Liang, J. P. Best, M. P. van Koeverden, G. K. Such, J. Cui and F. Caruso, *Science*, 2013, **341**, 154.

5 J. Saiz-Poseu, J. Sedó, B. García, C. Benaiges, T. Parella, R. Alibés, J. Hernando, F. Busqué, and D. Ruiz-Molina, *Adv. Mater*., 2013, **25**, 2066.

6 Q. Zou, L. Zhang, X. Yan, A. Wang, G. Ma, J. Li, H. Mçhwald and S. Mann, *Angew. Chem. Int. Ed*., 2014, **53**, 2366.; M. Li, D. C. Green, J. R. Anderson, B. P. Binks and S. Mann, *Chem. Sci*., 2011, **2**, 1739.

RSC Advances Accepted Manuscript

7 C. Wang, Y. Guo, Y. Wang, H. Xu, R. Wang and X. Zhang, *Angew. Chem. Int. Ed.*, 2009, **48**, 8962.; X. Zhang, Z. Chen and F. Würthner, *J. Am. Chem. Soc*., 2007, **129**, 4886.; P. Long and J. Hao, *Soft Matter*, 2010, **6**, 4350.; L. Jiang, Y. Peng, Y. Yan and J. Huang, *Soft Matter*, 2011, **7**, 1726.; X. Yan, S. Li, T. R. Cook, X. Ji, Y. Yao, J. B. Pollock, Y. Shi, G. Yu, J. Li, F. Huang and P. J. Stang, *J. Am. Chem. Soc*., 2013, **135**, 14036.

8 J. H. Magill, *J. Mater. Sci*., 2001, **36**, 3143.

9 Y. Su, W. Liang. W. Jin, H. Zhang and G. Liao, *Acta Optica Sinica*, 2007, **27**, 1239.

10 A. G. Shtukenberg, Y. O. Punin, E. Gunn and B. Kahr, *Chem. Rev*., 2012, **112**, 1805.

11 P. Divry and M. C. R. Florkin, *Soc. Biol*., 1927, **97**, 1808.; G. Kelenyi, *Acta Neuropathol*. 1967, **7**, 336.

12 (a) R. H. Fung Cheung, J. G. Hughes, P. J. Marriott and D. M. Small, *Food Chem*., 2009, **112**, 507; (b) S. Salmaso, A. Semenzato and P. Caliceti, *Bioconjugate Chem*., 2004, **15**, 997; (c) P. Garin-Chesa, I. Campbell, P. E. Saigo, J. L. Jr. Lewis, L. J. Old and W. Rettig, *J. Am. J. Pathol.*, 1993, **142**, 557; (d) H. Wang, C. Yang, L. Wang, D. Kong, Y. Zhang and Z. Yang, *Chem. Commun*., 2011, **47**, 4439; (e) L. Perez-Alvarez, V. Saez-Martinez, E. Hernaez, M. Herrero and I. Katime, Macromol. *Chem. Phys*., 2009, **210**, 467; (f) S. Nayak, H. Lee, J. Chmielewski and L. A. Lyon, *J. Am. Chem. Soc*., 2004, **126**, 10258; (g) T. Kato, T. Matsuoka, M. Nishii, Y. Kamikawa, K. Kanie, T. Nishimura, E. Yashima, and S. Ujiie, *Angew.*

RSC Advances Accepted Manuscript

Chem. Int. Ed., 2004, **43**, 1969; (h) N. Sakai, Y. Kamikawa, M. Nishii, T. Matsuoka, T. Kato and S. Matile, *J. Am. Chem. Soc*., 2006, **128**, 2218.

13 (a) P. Chakraborty, B. Roy, P. Bairi and A. K. Nandi, *J. Mater. Chem*., 2012, **22**, 20291.; (b) P. Xing, X. Chu, M. Ma, S. Li and A. Hao, *Phys. Chem. Chem. Phys*., 2014, **16**, 8346.; (c) P. Xing, X. Chu, G. Du, M. Li, J. Su, A. Hao, Y. Hou, S. Li, M. Ma, L. Wu and Q. Yu, *RSC Adv*., 2013, **3**, 15237.

14 (a) Z. Shen, T. Wang and M. Liu, *Chem. Commun*., 2014, **50**, 2096.; (b) S. Manna, A. Saha and A. K. Nandi, *Chem. Commun*., 2006, 4285.

15 For example: B. Roy, P. Bairi, and A. K. Nandi, *RSC Adv*., 2014, **4**, 1708.; S. Chatterjee and A. K. Nandi, *Chem. Commun.*, 2011, **47**, 11510.; A. Saha, B. Roy, A. Garai, and A. K. Nandi, *Langmuir*, 2009, **25**, 8457.

16 H. Bai, C. Li, X. Wang and G. Shi, *J. Phys. Chem. C*, 2011, **115**, 5545.

17 L. Gránásy, T. Pusztai, G. Tegze, J. A. Warren and J. F. Douglas, *Phys. Rev. E*, 2005, **72**, 011605.

18 M. M. Piepenbrock, G.O. Lioyd, N. Clarke and J. W. Steed, *Chem. Rev*., 2010, **110**, 1960.

19 S. Yagai, M. Yamauchi, A. Kobayashi, T. Karatsu, A. Kitamura, T. Ohba and Y. Kikkawa, *J. Am. Chem. Soc*., 2012, **134**, 18205.

20 P. Bairi, B. Roy, and A. K. Nandi, *J. Phys. Chem. B*, 2010, **114**, 11454.

21 C. Zhan, P. Gao and M. Liu, *Chem. Commun*., 2005, 462.

22 M. Wang, A. R. Mohebbi, Y. Sun, and F. Wudl, *Angew. Chem. Int. Ed.*, 2012, **51**, 6920–6924. (μ_N is the standard part of the chemical potential or the mean interaction

RSC Advances Accepted Manuscript

free energy of one molecule in aggregates; N stands for aggregation number; μ_∞ is the "bulk" energy of a molecule in an infinite aggregate; α is a constant dependent on the strength of the intermolecular interactions; T is temperature; k is Boltzmann constant).

RSC Advances Accepted Manuscript

Utilizing the self-assembly of folic acid/melamine complexes in water, we realized the construction of spherulites and networks with porous structure from membrane growth and folding.

RSC Advances Accepted Manuscript